eISSN: 2976-1190

Journal of Engineering and Sciences

Vol. 4, Issue 2, Nov 2025, 186-194

DOI: https://doi.org/10.3126/jes2.v4i2.86327

Journal homepage: Journal of Engineering and Sciences (nepjol.info)

Publisher: Research Management Cell, Pashchimanchal Campus, Lamachour, Pokhara

Comparative Analysis of Horizontal Axis Wind Turbine Rotors with and without a winglet at various wind speeds using Computational Fluid Dynamics Approach

Ashim Chhetri [1,*], Aayus Pandey[1], Gaurav Lamsal[1], Bijaya Dharel[1], Nishan Subedi[1], Pawan C. Awasthi[1], Dipesh Karki[1,*]

[1]*Department of Mechanical and Automobile Engineering, IOE, Pashchimanchal Campus, T.U.*

**Corresponding Author:* ashimchhetr@gmail.com *,dipeshk@wrc.edu.np*

(Manuscript Received: 29/04/2025; Revised: 11/11/2025; Accepted: 00/11/2025)

Abstract

This project investigates the aerodynamic performance of a Horizontal Axis Wind Turbine (HAWT) blade using NREL S-series airfoils (S830, S831, S832) with and without a winglet at various wind speeds. The blade was designed in QBlade and modeled in SolidWorks, with simulations performed in ANSYS Fluent using a steady-state RANS approach and the SST k–ω turbulence model. A winglet was added to the blade tip to assess its effect on performance. The computational domain applied the Multiple Reference Frame (MRF) to simulate rotating effects. Results show that the winglet improves power output by up to 3.55% at low wind speeds, with smaller gains at higher speeds. Comparative torque analyses and mesh-independence tests were performed to validate numerical accuracy. This suggests that winglets help reduce energy losses and improve turbine performance, especially at lower wind speeds.

Keywords: CFD, Horizontal Axis Wind Turbine, NREL, Winglet

Introduction

Wind energy is a fast-growing renewable energy source that plays a key role in reducing dependence on fossil fuels and combating climate change. HAWTs are the most used because of their high efficiency and flexible design. HAWTs have a horizontal rotor shaft mounted atop a tall tower, with blades facing the wind to capture its energy and convert it to electricity using a generator. The nacelle (the box behind the blades) houses key components such as the wind vane, anemometer, controller, and yaw motor. These components help turn the blades toward the wind and, in strong winds, protect the system through braking systems. The blades, usually made of fiberglass, are shaped along their length using special airfoil designs to improve efficiency. Key airfoil features—such as chord length, camber, thickness, and angle of attack—play an important role in the blade's aerodynamic performance.

Blade design and testing are often done using QBlade, a free software tool based on Blade Element Momentum (BEM) theory. QBlade allows users to choose airfoils, define the blade shape along its length, and simulate its performance. BEM theory breaks the blade into small sections to analyze forces such as lift and drag, while accounting for losses near the blade tips and root (Sayed et al., 2012).

Extra design features, such as winglets on the blade tips, help reduce drag and minimize energy losses due to swirling airflow, thereby improving overall performance (Najar & Harmain, 2013). One important factor is the Tip Speed Ratio (TSR), the ratio of the blade tip speed to the wind speed. Choosing the right TSR helps get the most energy from the wind. Another critical factor is the Reynolds number, which helps describe how air flows over the blade, whether it is in a smooth (laminar) or mixed (turbulent) flow.

To understand how air flows around the blades in more detail, engineers use Computational Fluid Dynamics (CFD). The RANS model, especially with the SST k–ω turbulence model, is commonly used to simulate airflow accurately (Mahawadiwor et al., 2012). ANSYS Fluent is a popular CFD software that helps analyze how air moves, how heat is transferred, and how efficient the turbine design is. This study uses both QBlade and ANSYS Fluent to study and evaluate how the wind turbine blade performs.

1. Materials and Methodology

1.1 Materials and tools

For performing numerical analysis, a 3D geometric model of the Wind turbine and a simulation were performed on scientific tools such as QBlade, SolidWorks, and ANSYS Fluent, respectively.

a) QBlade v0.6: BEM-based blade designing (Hasan et al., 2017).

b) ANSYS Fluent 2021 R1: Steady RANS CFD with SST k–ω and sliding mesh (Inc, 2021).

c) SolidWorks 2021: Airfoil lofting, blade exporting, and complete rotor assembly (Systèmes, 2021).

2.2 Methodology

The numerical analysis is conducted in several steps to complete the experiment, as shown in the following flowchart, in Figure 1. Initially, the various design considerations of the wind turbine were studied. The numerical modeling and analysis are conducted using the CFD software ANSYS Fluent. Simulations are performed to investigate torque as a function of wind velocity.

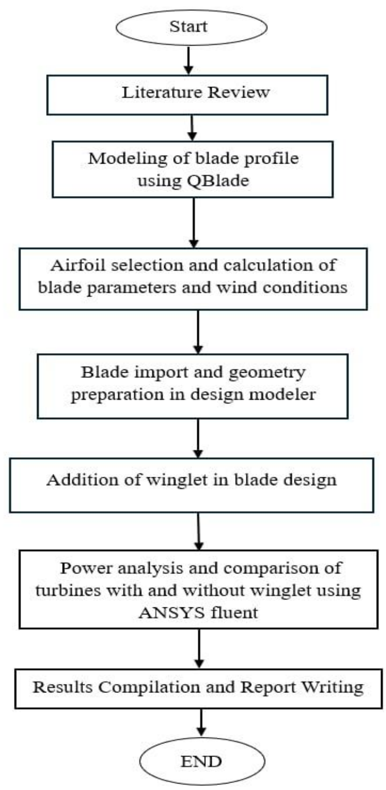

Figure 1: Flow diagram showing methodology

2.2.1 Blade Length Calculation

The blade length is calculated from the following procedure:

Considerations:
ρ= 1.240 kg/m3, v= 10m/s,
C_p=0.3

P_{output} = 100kW
k_w = 5%
k_m = 0.2%
k_e = 1.5%
$k_{e,t}$ = 5%
k_t = 3%
$\mu' = (1-k_m)\times(1-k_e)\times(1-k_{e,t})\times(1-k_t)\times(1-k_w)\times C_p$
μ'= 0.258
$P_{output} = \mu\times P_{wind}$ ($\therefore P_{wind} = 0.5\times\rho\times v^3\times\pi\times R^2$)
R = 14.540m
R ≈ 15m.

2.2.2 Chord Length calculation

Several theories exist for determining the optimal chord length, which can provide an initial approximation for each blade section. Among these, the theory presented in Wind Turbine Technology: Principles and Design by Muyiwa Adaramola (Adaramola, 2014) offers the following formulae for calculation.

$$C(r) = \frac{2\pi r}{n}\frac{8}{9C_L}\frac{U_{wd}}{\lambda_r V_r} \qquad (1.1)$$

where,

$$Vr = \sqrt{V_w^2 + U^2} \qquad (1.2)$$

The average of C(r) is obtained as 1.23.

2.2.3 Airfoil selection

By conducting multiple sets of experiments, NREL has classified airfoil families comprising 35 airfoils for various-sized rotors since 1984 (Tangier & Somers, 1995). NREL has specified various combinations of airfoils to achieve optimal performance. The selection of a combination of S830, S831, and S832 from root to tip by analyzing different experiments and various papers by NREL (Airfoiltools. n.d. S830-NR; S831-NR; S832-NR).

2.2.4 Rotational speed calculation

A 3-blade wind turbine works most efficiently when its tip speed ratio (TSR) is between 6 and 8 (Tangler & Somers, 2012). This range gives a good mix of performance and durability. If the TSR is below 6, the blades spin too slowly, making them less efficient because of greater air resistance and insufficient lift (Ingram, 2011). On the other hand, if the TSR is greater than 8, the blades spin too fast, which can put too much strain on them, increase noise, and cause wear to accelerate. It can also reduce efficiency due to more drag and air turbulence. So, choosing a TSR of 7 is a good middle ground (Jamieson, 2011).

2.2.5 Blade Modelling

The airfoil analysis data were obtained from airfoil tools, in which the airfoil profiles were sized, shaped, and twisted using 360-degree polar extrapolations, built-in programs, and codes. Thus, the coordinates of the blade profile were extracted in SOLIDWORKS. Then, from the curves, a single blade is prepared using a loft tool. Then, the hub design, assembly, and all other adjustments are entirely done in SOLIDWORKS.

2.2.6 Addition of a winglet to the blade geometry

In this study, the winglet design is based on three main factors: height, cant angle, and curvature radius. The focus is on how changes in height and curvature radius affect the wind turbine's performance. The selected design uses a winglet height of 900 mm (2.5% of the rotor radius), a curvature radius of 200 mm (1.2% of the rotor radius), and a fixed cant angle of 90°.

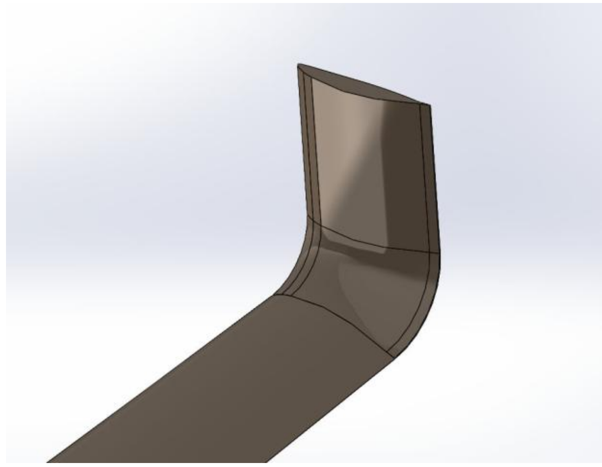

Figure 2: Winglet attachment on blade geometry

2.2.7 Geometry preparation

The simulation area is a 3D rectangular space made up of two parts: a rotating circular section around the wind turbine blades and a fixed outer section. The rotating part is used to capture the changing aerodynamic behavior caused by the spinning rotor, while the stationary part allows air to flow in and out properly.

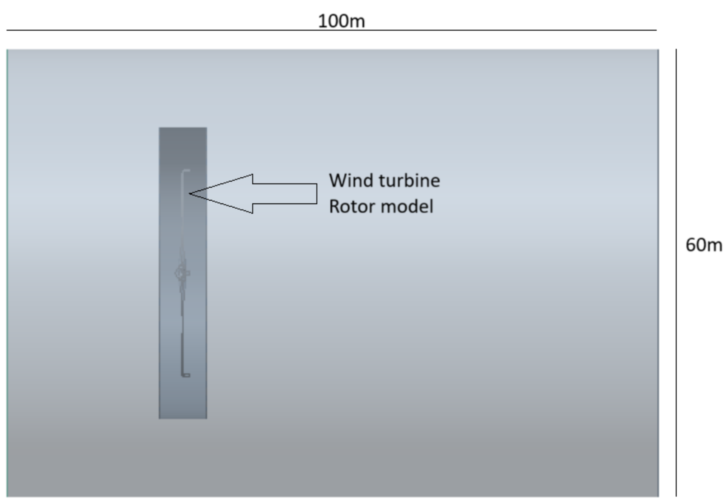

Figure 3: Side view of the Computational model

2.2.8 Meshing

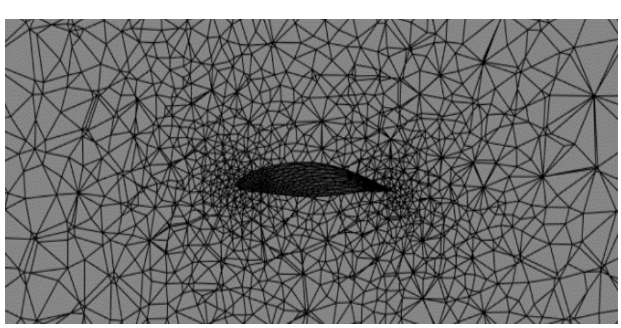

Figure 4: Meshing

Meshing is an essential step in CFD, dividing complex geometry into smaller elements for accurate simulation. For a mesh size of 1.5, as shown in Figure 2, quality was evaluated using skewness, orthogonality, and element quality. Skewness ranged from 2.231e-007 to 0.82971, staying within an acceptable limit.

2.2.9 Analysis Settings and Boundary Conditions

In this study, a steady-state, pressure-based solver was used to simulate incompressible flow with gravity set at 9.81 m/s². The SST k-ω turbulence model with wall treatment was selected for its effectiveness in capturing boundary layer behavior, especially in rotating domains. The computational domain included a rotating solid zone at various RPMs and a stationary fluid zone. Velocity inlets ranging from 1 to 16 m/s and a pressure outlet were applied as boundary conditions. The SIMPLE algorithm was used for pressure-velocity coupling, with second-order accuracy for pressure and momentum equations to ensure solution precision.

2.2.10 The governing equations of the Multiple Reference Frame (MRF) approach

The Multiple Reference Frame (MRF) approach in Computational Fluid Dynamics (CFD) is a steady-state method used to simulate flows involving rotating components, such as fans, impellers, or turbines, without requiring a full transient (time-dependent) simulation. In this method, the computational domain is divided into different zones: rotating zones, where the flow equations are solved in a rotating frame of reference, and stationary zones, where the standard Navier–Stokes equations are applied. Within the rotating zones, the governing momentum equation is modified to account for rotational effects by including additional source terms: the Coriolis force and the centrifugal force. The modified momentum equation becomes:

$$\frac{\partial \vec{u}}{\partial t} + (\vec{u} \cdot \nabla)\vec{u} = -\frac{1}{\rho}\nabla p + \nu\nabla^2\vec{u} - 2\vec{\Omega} \times \vec{u} - \vec{\Omega} \times (\vec{\Omega} \times \vec{r}) \ldots (1)$$

2.2.11 Solver Model

The K-ω SST (Shear Stress Transport) model is a widely used turbulence model in CFD that accurately predicts flow separation and near-wall turbulence. It blends the k-ω model near the surface with the k-ε model in the outer flow, making it suitable for complex flows like those around a wind turbine blade.

2.2.12 Mesh Independence Test

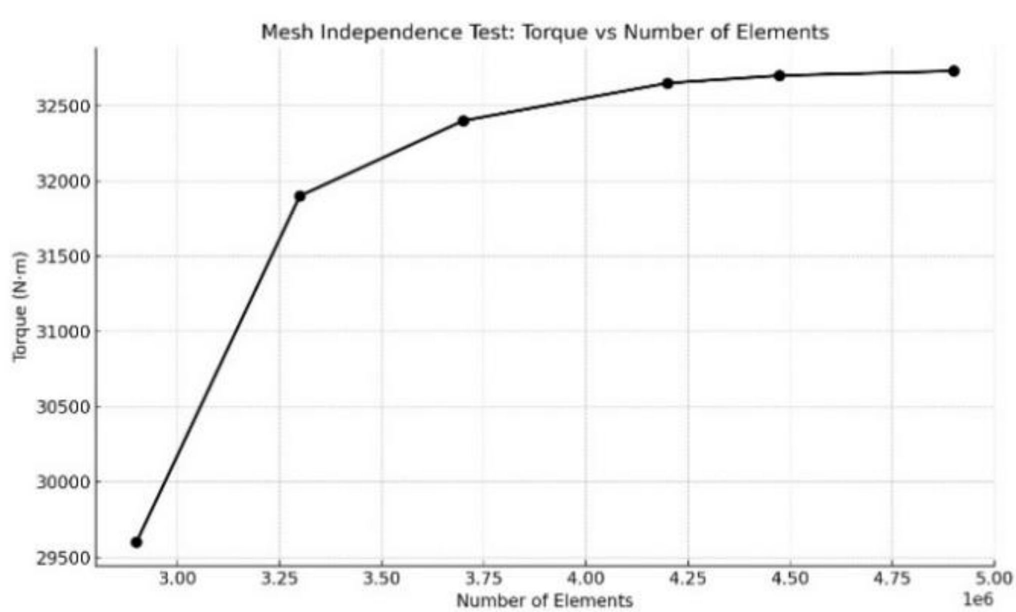

Figure 5: Torque vs Number of elements graph

A mesh independence test was performed to ensure the simulation results are not influenced by mesh size. The graph shows that torque increases with mesh refinement but stabilizes beyond approximately 4.4 million elements. At 4,474,215 elements, there is no significant change in torque, indicating mesh independence. Therefore, this mesh size was selected for the final analysis.

2. Results

Fluids naturally move from areas of high pressure to low pressure, and this basic principle is used in turbines to generate mechanical energy. As the fluid flows through the turbine, its pressure energy is converted into rotational motion, which is then used to produce power. The pressure difference drives this movement, as the fluid attempts to balance out the pressure gradient. In a rotating system like a wind turbine, the motion of the blades helps draw in the incoming air and push it through, improving airflow and energy conversion efficiency. As the turbine extracts energy from the wind, the wind slows as it passes through the rotor.

3.1 Wind Turbine Model without Winglets

Torque increases with wind velocity for both the numerical results without a winglet and the theoretical values. Theoretical torque remains higher across all velocities, indicating an overestimation compared to the more realistic numerical results. As velocity increases from 2 to 16 m/s, the gap between theoretical and numerical torque also widens, suggesting that aerodynamic losses and inefficiencies become more pronounced at higher speeds.

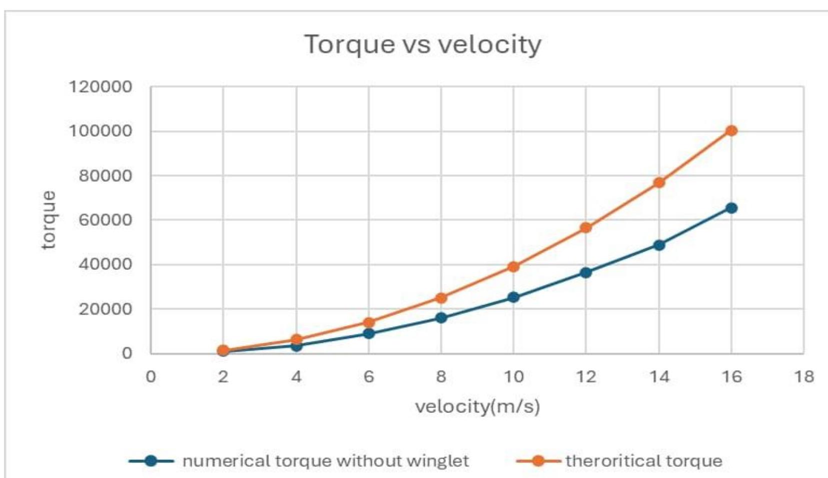

Figure 6: Torque vs wind velocity graph without winglets

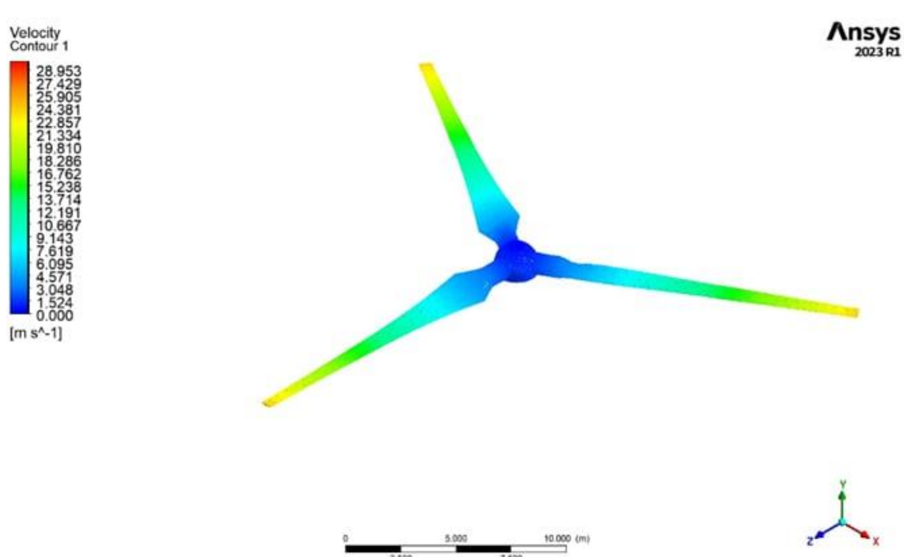

Figure 7: Velocity contour of wind turbine blade without winglets at 4m/s

3.2 *Wind turbine model with winglets*

Torque increases steadily with velocity for both the theoretical case and the simulation with the winglet. The torque values with winglets remain lower than the theoretical values across all velocities, though the difference is slightly reduced compared to cases without winglets. This indicates that winglets improve performance by reducing energy losses and enhancing aerodynamic efficiency. However, some gaps remain due to real-world effects such as drag and turbulence, which are not captured by the theoretical model.

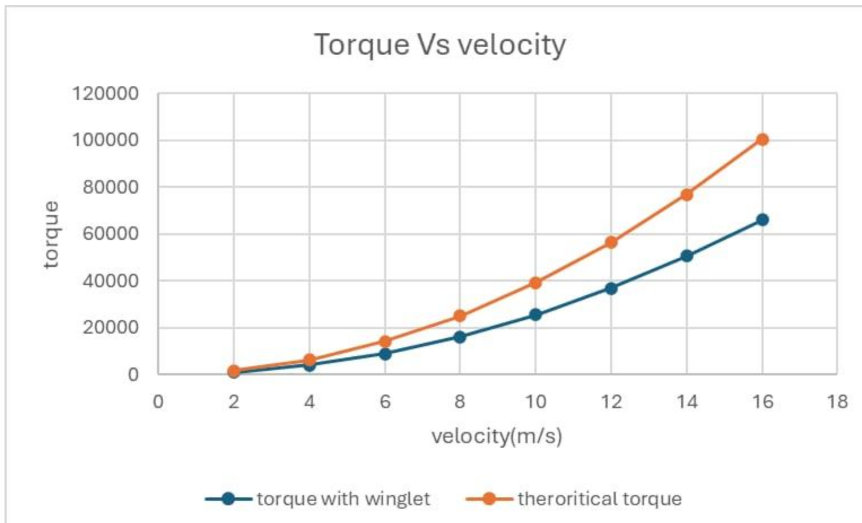

Figure 8: Torque vs wind velocity graph with winglets

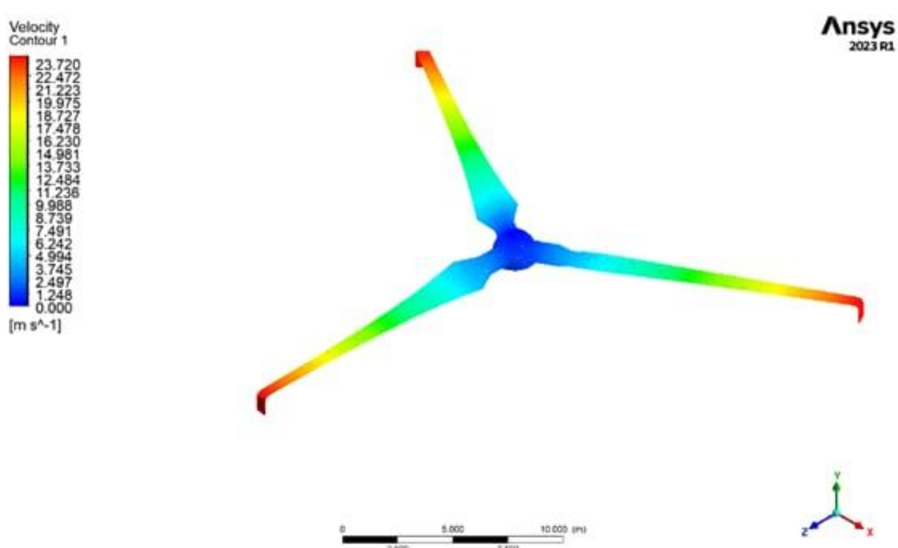

Figure 9: Velocity contour of wind turbine with winglets at 4m/s

3. Conclusions

The analysis shows that adding a winglet to the HAWT slightly increases power output at all wind speeds. The power gain ranges from 0.77% to 3.55%, with the highest increase at 16 m/s. As wind speed increases, the percentage decreases, meaning winglets are more effective at lower speeds. Though the improvement is small, winglets help reduce tip losses and improve efficiency. With better design, winglets could give more benefits at higher wind speeds.

4. Acknowledgement

We are genuinely grateful to RMU Pashchimanchal Campus for enabling us to participate in a project that will significantly enhance our research capabilities in a subject we are incredibly passionate about.

References

[1] Sayed, M. A., Kandil, H. A., & Shaltot, A. (2012). Aerodynamic analysis of different wind-turbine-blade profiles using finite-volume method. *Energy Conversion and Management, 64*, 541–550. https://doi.org/10.1016/j.enconman.2012.05.030

[2] Najar, F. A., & Harmain, G. A. (2013). Blade design and performance analysis of a wind turbine. *International Journal of ChemTech Research, 5*(2), 1054–1061.

[3] Mahawadiwar, H. V., Dhopte, V. D., Thakare, P. S., & Askhedkar, R. D. (2012). CFD analysis of wind turbine blade. *International Journal of Engineering Research and Applications, 2*(3), 3188–3194.

[4] Hasan, M., El-Shahat, A., & Rahman, M. (2017). Performance investigation of three combined airfoils bladed small scale horizontal axis wind turbine by BEM and CFD analysis. *Journal of Power and Energy Engineering, 5*(5).

[5] ANSYS Inc. (2021). *Fluent theory guide*.

[6] Dassault Systèmes. (2021). *SolidWorks user guide*.

[7] Adaramola, M. S. (n.d.). *Wind turbine technology*. CRC Press.

[8] Tangier, J. L., and D. M. Somers. 1995. *NREL Airfoil Families for HAWTs.* NREL/TP-442-7109. Golden, CO: National Renewable Energy Laboratory. https://docs.nrel.gov/docs/legosti/old/7109.pdf.

[9] Airfoiltools (n.d.). *S830-NR airfoil data*. Retrieved July 30, 2025, from http://airfoiltools.com/airfoil/details?airfoil=s830-nr

[10] AirfoilTools (n.d.). *S831-NR airfoil data*. Retrieved July 30, 2025, from http://airfoiltools.com/airfoil/details?airfoil=s831-nr

[11] AirfoilTools (n.d.). *S832-NR airfoil data*. Retrieved July 30, 2025, from http://airfoiltools.com/airfoil/details?airfoil=s832-nr

[12] Tangler, J. L., & Somers, D. M. (2012). *Quiet airfoils for small and large wind turbines* (Patent US 8,197,218). U.S. Department of Energy / National Renewable Energy Laboratory.

[13] Ingram, G. (2011). *Wind turbine blade analysis using the blade element momentum method* (Version 1.1).

[14] Jamieson, P. (2011). *Innovation in wind turbine design*. Wiley.